Structural Eng./Earthquake Eng., JSCE, Vol. 19, No. 2, 65s—80s, 2002 July
(J. Struct. Mech. Earthquake Eng., JSCE, No. 710/ I —60)

FATIGUE PERFORMANCE OF COMPOSITE TUBULAR K-JOINTS FOR TRUSS TYPE BRIDGE

Pison UDOMWORARAT[1], Chitoshi MIKI[2], Atsushi ICHIKAWA[3], Masanori KOMECHI[4]
Kaoru MITSUKI[5] and Tetsuya HOSAKA[6]

[1]Member of JSCE, Dr.Eng., Graduate Student, Dept. of Civil Eng., Tokyo Institute of Technology
[2]Fellow of JSCE, Dr.Eng., Professor, Dept. of Civil Eng., Tokyo Institute of Technology
[3] Fellow of JSCE, Dr.Eng., Manager, Research and Development Promotion Division, Railway Technical Research Institute
[4]Member of JSCE, M.Eng., Graduate Student, Dept. of Civil Eng., Tokyo Institute of Technology
(2-12-1, O-Okayama, Meguro-ku, Tokyo 152-8552, Japan)
[5]Member of JSCE, Corporate Planning Dept., Japan Railway Construction Public Corporation
[6]Member of JSCE, Dr.Eng., Design & Technology Dept., Railway Engineering Corporation
(2-14-2, Nagata-cho, Chiyoda-ku, Tokyo 100-0014, Japan)

The structural performances of composite tubular K-joint leading to real truss bridge construction of high speed Shinkansen train are presented. The experimental studies on improving the fatigue performance of welded steel tubular joints by upgrading the structural joint details and improving the weld toe profiles were carried out on ten tubular K-joints under repeated constant amplitude load. The behaviour of all joints were examined through the analyses and the tests. The results suggest that concrete filled tubular joints are able to improve the fatigue strength substantially compared to unfilled joint.

Key Words *: composite tubular K-joints, fatigue strength, stress concentration*

1. INTRODUCTION

Steel tubular members are widely used in various structures[1),2)], such as offshore structures, power towers and building structures due to their attractive properties; e.g., good post-buckling behavior, excellent properties in strength and economical advantage. Structures made of circular section have been proven to be the best shape for elements subjected to wind-, water- or wave-loadings because they offer favorable aerodynamic and hydrodynamic properties. A smaller surface area as compared to the structures made of open sections and an absence of sharp corners result in a better performance of corrosion protection[3)].

In this study, tubular K-joints have been studied in order to apply to a truss bridge[4),5)] used for the high speed train system (Shinkansen) as shown in **Fig.1**. The use of tubular members instead of the usual box or H-shape section members can reduce construction and maintenance cost while offering the same service structural performance levels; i.e., reduction in material usage, painting areas and welding details[6)].

However, at some particular connections of the chords and the diagonal members, fatigue can limit the overall structural performance because of localized high stress concentration caused by local bending and membrane stresses[7)-10)]. The fatigue strength near the welded region is quite sensitive to the stress concentration[11)]. The stresses in this critical region can vary greatly because of global and local geometric parameters, overall connection configuration, tube diameter, wall thickness, stiffener details and even weld bead profiles.

In order to reduce the localized high stress concentration, the simple joints were partially filled with concrete. Various types of concrete filled tubular joints[12)-15)] have been examined. Those were: (1) joint filled with concrete inside the chord solely, (2) joint filled inside both the chord and the diagonals, (3) joint filled inside both the chord and the diagonals combined with perfobond stiffeners (steel rib plates with providing through thickness holes). These improved joints are expected to apply to the bridge structure at the joint region exclusively. The lengths of tube remote from the joint are to remain hollow. This is done to minimize the increase in dead weight of the members.

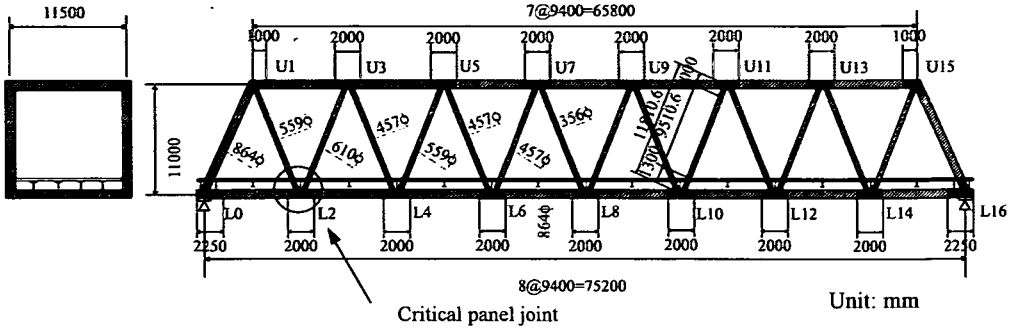

Fig.1 Tubular truss bridge

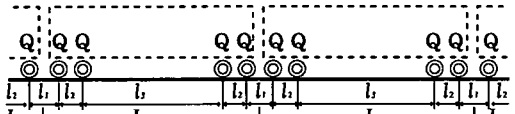

Load/axle Q \ Length (m)	L	l_1	l_2	l_3
17 tons	20.0	3.5	2.2	12.1

Fig.2 Train load pattern

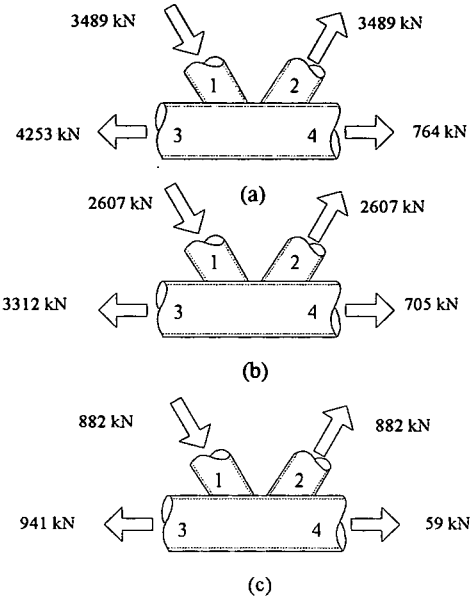

Fig.3 Loading mode

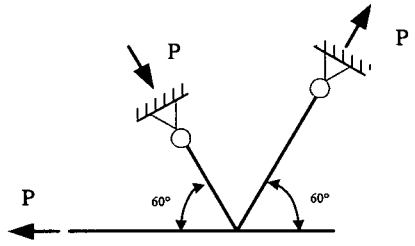

Fig.4 Forces in test specimen

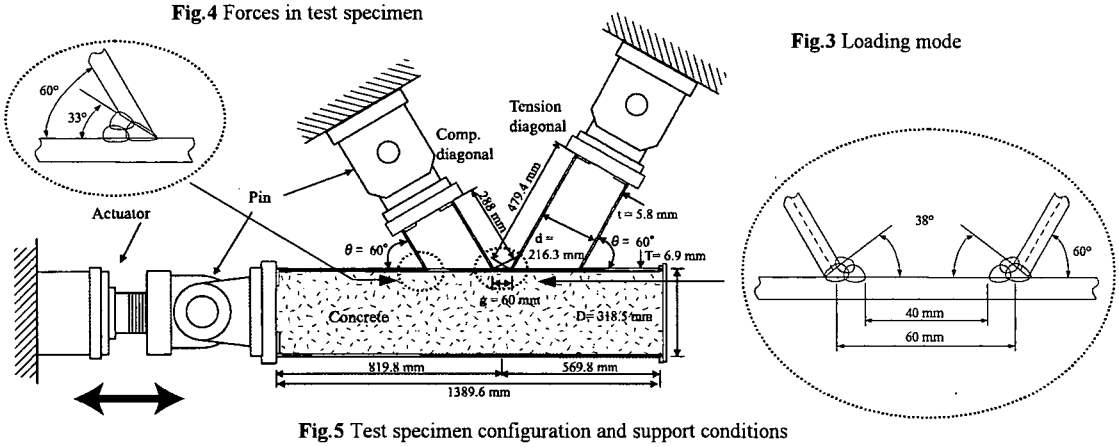

Fig.5 Test specimen configuration and support conditions

2. MODEL BRIDGE AND LOADING MODE

Fig.1 shows the model bridge of this study. The bridge was designed as a simply supported structure, made up of two main warren-type trusses. It has a span of 75.2 m, a height of 11 m and a width of 11.5 m. The distance between the panel points is 9.4 m. The diagonal members connect the upper and lower chords 60° inclination. The concrete is filled at the

Table 1 Mechanical properties of steel

STK400	Yield strength (MPa)	Ultimate strength (MPa)	Elongation (%)
Chord	379	432	35
Diagonal	369	459	32

Table 2 Concrete properties of test specimens

Filled concrete	Compressive strength at 28 days (MPa)
Ordinary concrete I	26.3
Super-light weight	29.4

joint portion as shown in **Fig.1**. The length of filled concrete of each chord is almost the same as the diameter of the chord.

Preliminary analysis led the outer chord diameter of 864 mm and wall thickness varying from 12 to 38 mm. The outer diagonal diameter and the thickness were varied from 365 to 610 mm and 11 to 29 mm, respectively, depending on resisting force in each member.

According to the design specifications of railway bridge[16], Shinkansen P-17 load pattern was adopted and used to determine nominal stress influence lines of the bridge. **Fig.2** illustrates the P-17 load pattern of the train. In addition, an impact load was imposed to live loads. As a result, the loads on each axle increased about 13.6%.

Three-dimensional frame finite element analyses were employed to examine the truss bridge. The analyses pointed out that some particular panel joint might be subjected to enough high nominal stress variation in diagonal members to cause fatigue problem. This critical joint was found to be the joint near the support (L2) as shown in **Fig.1** and it was adopted as a representative tubular joint in this study.

Fig.3(a) and **Fig.3(b)** show the force equilibrium conditions corresponding to two loading modes that give the highest stress variation at the critical joint (L2). The joint was subjected predominantly to the applied axial forces where the secondary bending moment had less influence on the joint. **Fig.3(c)** shows the variation of the forces in the members by subtracting the forces in **Fig3(b)** from **Fig.3(a)**. From **Fig.3(c)**, the results suggested that the change of the forces contributed to the critical joint predominantly coming from member 1, 2 and 3 where member 4 seemed to have a little contribution compared with the other three members.

Set-up of test specimen was considered to simulate the actual behavior of the critical joint under the loading conditions. In this way, the loading mode was simplified as a simple K-joint

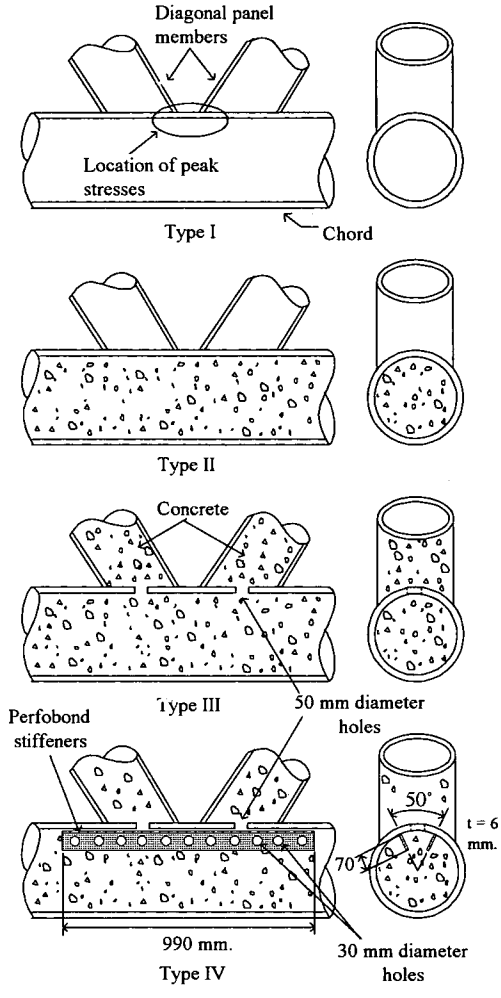

Fig.6 Composite tubular K-joint details

subjected to the axial force at the chord left end whereby connecting both diagonals with pin supports as shown in **Fig.4**. Proportional forces in each member will be induced. This simple set-up, which able to be applied on the cellular test floor system, could effectively simulate the critical joint Finally, the specimen was set as illustrated in **Fig.5**.

3. SPECIMEN TYPES AND TESTING METHOD

Four types of the tubular K-joints were considered in this study. Each had the same exterior dimensions and geometry, only the interior details were different in order to provide a better structural performance. The 4 types of the prototype joints could be fabricated as shown in **Fig.6**. All the joints were about $^1/_3$-scale of the actual structural size. The

Table 3 Fatigue test specimens

Type	Specimen	Applied load range (kN)	Nominal stress range in tension diagonal (MPa)	Weld toe treatment	Concrete type	Fatigue life ($\times 10^5$) cycles		
						N_c	N_{20}	N_f
I	KF-1	9.8-196 (1-20 tons)	47.3	Grind	-	0.75	4.5	7.6
I	KF-3	9.8-127.4 (1-13 tons)	29.7	Grind	-	3.0	7.0	51.0* →
		9.8-166.7 (1-17 tons)	39.8			→	→	19.7
II	KF-2	9.8-196 (1-20 tons)	47.3	Grind	Ordinary concrete I	9.0	9.0	50.3
II	KF-4	9.8-166.7 (1-17 tons)	39.8	Grind	Ordinary concrete I	→ No crack →		46.5* →
		9.8-245 (1-25 tons)	59.7			3.0	3.0	52.0
III	KF-6	9.8-303.8 (1-31 tons)	77.2	As-weld	Super-light weight	2.0	4.0	7.0
III	KF-7	9.8-196 (1-20 tons)	47.3	As-weld	Super-light weight	7.0	14.0	30.4
III	KF-9	9.8-196 (1-20 tons)	47.3	Grind	Super-light weight	→ No crack →		50.0* →
		9.8-245 (1-25 tons)	59.7			→ No crack →		30.0* →
		9.8-274.4 (1-28 tons)	67.2			3.0	3.5	6.0
IV	KF-5	9.8-343 (1-35 tons)	84.6	As-weld	Super-light weight	3.9	3.9	3.9
IV	KF-8	9.8-196 (1-20 tons)	47.3	As-weld	Super-light weight	15.0	19.0	55.0
IV	KF-10	9.8-245 (1-25 tons)	59.7	Grind	Super-light weight	21.0	25.0	39.0

Note: *Retest.

material of the specimens was STK400 of which mechanical properties are given in **Table 1**.

Type I joint represents basic K-joint without any improvement of the joint details. The joints were fabricated by using 216.3 mm diameter diagonals connected to one side of a 318.5 mm diameter chord. The inclined diagonals were full-penetrated welded around intersection circumferences on the chord 60 and 120 degrees from the horizontal level. The gap between both diagonals including weld leg lengths was approximately about 40 mm as shown in **Fig.5.**

Type II joint is identical to Type I joint except that concrete was completely filled inside the chord. This aimed at decreasing the chord ovalization due to the bending of the chord wall, and thus, resulted in a decrease in the stress concentration.

Type III joint is identical to Type I joint, however, 50 mm diameter holes were made on the intersection areas of the chord and the diagonals. Concrete could pass through the holes and filled both the chord and the diagonals by pumping technique.

Type IV joint is identical to Type III except that two pieces of partial perfobond stiffener, size of 70×990×6 mm, were welded inside the chord with an inclined angle 50 degrees apart as shown in **Fig.6**. On the centerline of the stiffeners, 30 mm diameter through thickness holes were made to provide a composite action with the filled concrete.

Fatigue test comprised 10 specimens of tubular K-joint Type I, II, III and IV. There were two types of concrete used to fill inside the joints as shown in **Table 2**. The first type was ordinary concrete I, and it was filled in the specimens Type II. The second type was super-light weight concrete, which had 12.7 kN/m^3 of unit weight, 10 mm maximum aggregate size, and it was filled in the specimens Type III and IV. Fatigue tests were carried out a few months after placing concrete.

Many studies[8),17)] indicated that fatigue strengths of welded tubular K-joints increased considerably by grinding welded beads to a concave profile leading to lower stress concentration at the transition part between weld and base material. Hence, to identify the fatigue improvement, some specimens were ground around the weld of both chord and diagonal sides in order to compared with the as-welded joints.

The fatigue tests of all specimens were conducted under constant cyclic amplitude loading axially at the chord end through a hydraulics actuator with 490 kN (50 tons) force capacity as shown in **Fig.5**. Before the fatigue test started, the specimens were loaded a number of times to relieve any residual installation stress in the strain gauges. After the shaking down procedure, all strains were recorded at increments up to the shake down load.

Table 3 shows specimen type, label, applied load range, nominal stress range in tension diagonal, welding condition and concrete type corresponding to each specimen. Although the stress distributions around the weld circumference had been known and although it was perceived that the induced stresses could initiate fatigue crack, in some specimens higher level of applied load must be provided to make a crack propagation after a large number of

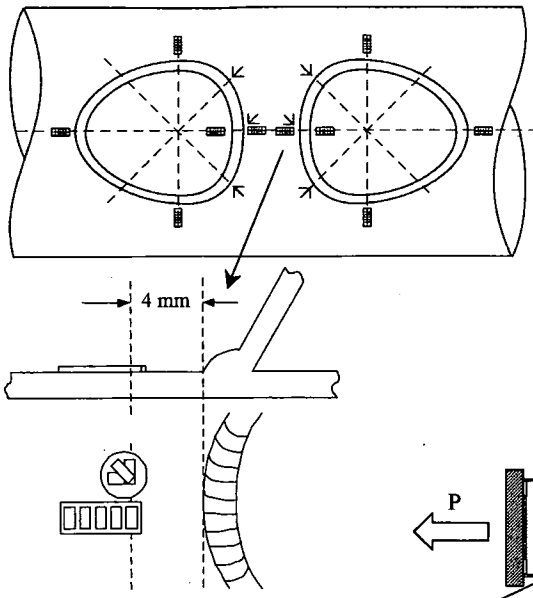

Fig.7 Arrangement of the gauges

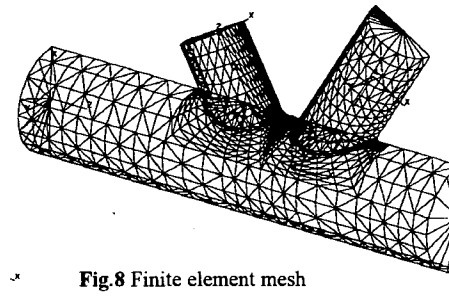

Fig.8 Finite element mesh

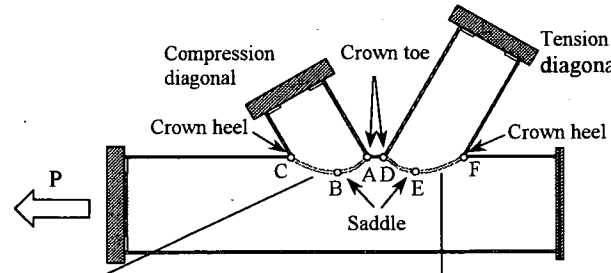

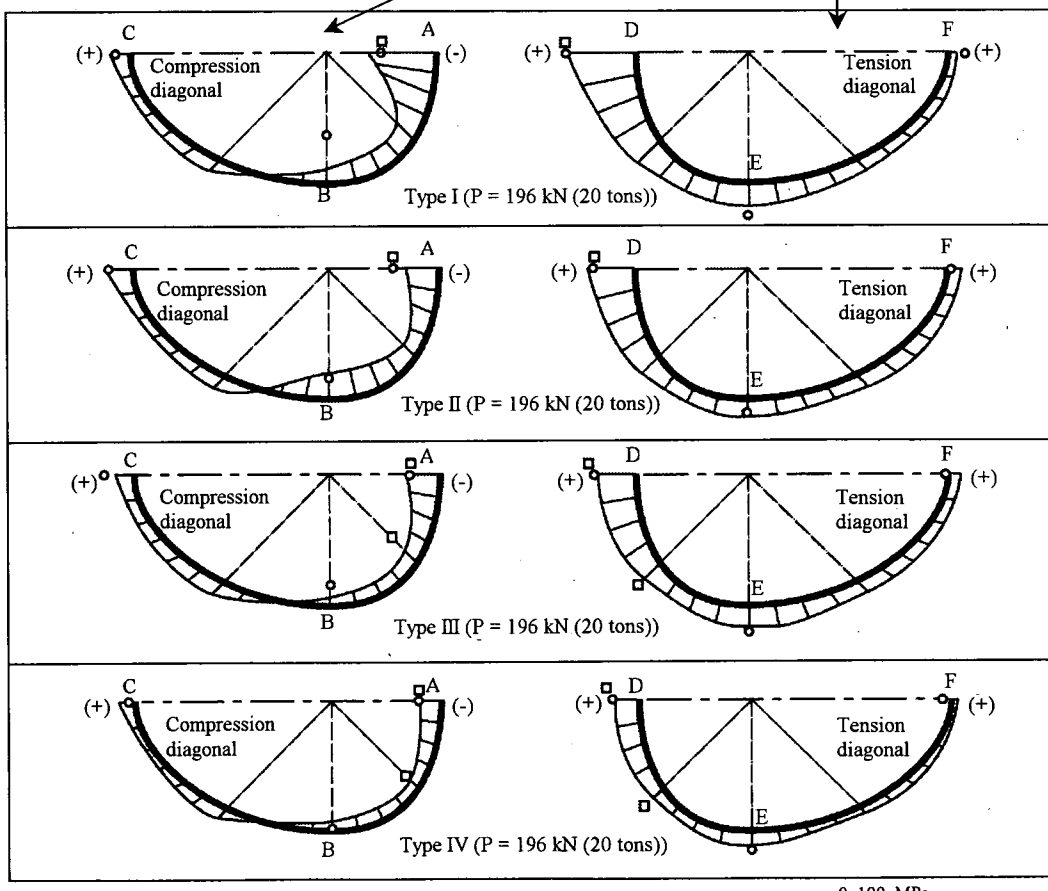

Fig.9 Distributions of maximum principal stress around the diagonals-chord intersection on exterior surface of the chord

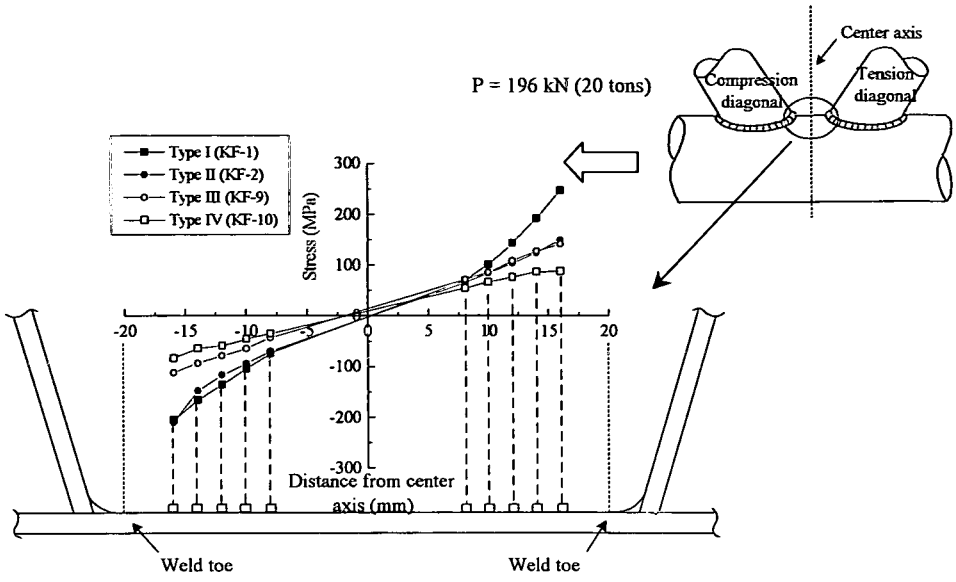

Fig.10 Stress distributions at the crown toe from gauge measurements

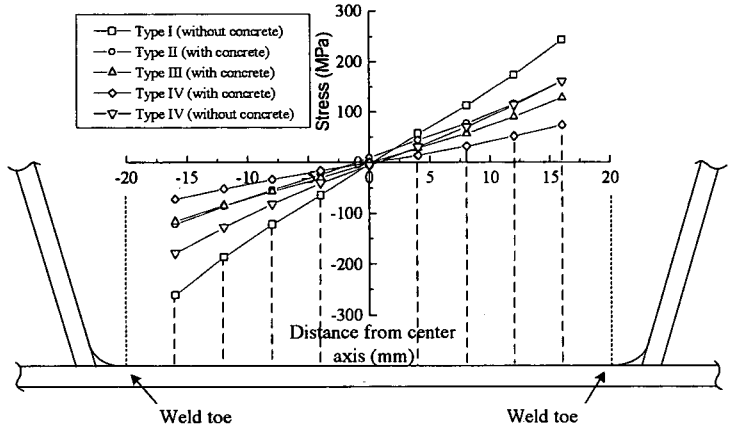

Fig.11 Stress distributions at the crown toe from FEM models

cycles without changing of crack length or an existing of the fatigue crack. Noted that, two steps of applied load range were applied on specimen KF-3 and KF-4 and three steps of applied load range were applied on specimen KF-9.

4. STRESS DISTRIBUTIONS

Stress distributions around weld intersection were investigated by FEM analyses and strain measurements. **Fig.7** illustrates an arrangement of strain gauges. The strain gauges of concentration type (1 mm in length) and rosette type (1 mm in length), were attached 4 mm away from the weld toe.

Three-dimensional nonlinear finite element analyses were carried out in order to investigate the behavior of the joints by using ABAQUS analysis code[18] as illustrated in **Fig.8**. The models have approximately 6000 elements where the smallest mesh size at the crown toe is 4 mm. The steel tube was modeled by using 3-nodes triangular shell element and the filled concrete was modeled by using tetrahedral 4-nodes and wedge 6-nodes solid elements. Inelastic material and geometrical nonlinear behavior were used for these elements. The steel behavior was assumed to be bilinear elastic-plastic model based on von Mises yield criteria defining the yield surface. The concrete behavior was assumed to use linear elastic model.

Young's modulus and Poisson's ratio of the steel and the concrete were 2.1×10^5 MPa and 0.3, and 2.5×10^4 MPa and 0.2, respectively.

In addition, the steel wall and the concrete were modeled by means of contact elements to simulate bonding between the interfaces. When the surfaces are in contact, normal forces develop between two materials, therefore, the transfer of compressive forces is possible. On the contrary, if the contact element is in tension, the contact surfaces separate from each other resulting in no bond develop. Eventually, the results from the finite element models were expected to correlate with the experimental results.

Fig.9 illustrates the measured and calculated maximum principal stresses on exterior surface of the chord 4 mm away from the weld toe. It is apparent that the maximum tensile and compressive local stresses of all joint types are at the crown toe on the chord wall between the tension and the compression diagonals. In addition, the stresses in the direction perpendicular to the weld toe are comparatively equal to the stresses in the principal direction. As expected, the stress distributions around the circumference are influenced considerably by the filled concrete and the perfobond stiffeners. The improved joint Type II, III and IV can reduce the stresses especially Type IV, in which the stresses around the circumference are much lower than the other types. The measured stresses agree well with the calculated ones.

To compare the reduction of the stresses, the measured stress distributions along the gap at the crown toe of all joint types are shown in **Fig.10**. The plot origin is located at center axis where the distance between the diagonals is equally divided. Comparisons of the stresses among specimen types are plotted based on 196 kN (20 tons) applied load basis. A significant decrease in the stresses of the improved joints compared to the hollow joint can be clearly observed from these plots. The obtained stresses from the first gauge reading of Type II joint (KF-2) is 60% as high of hollow joint Type I (KF-1) near tension diagonal. However, no discrepancy can be observed clearly near compression diagonal. Type III joint (KF-9) is 57% as high of the hollow joint near tension diagonal and 55% as high near compression diagonal. For Type IV joint (KF-10), the stresses are 35% near tension diagonal and 40% near compression diagonal of the hollow joint.

Fig.11 shows the stress distributions at the crown toe from the finite element models. Similarly, contributions of the concrete to reduce the stresses can be observed in Type II, Type III, and Type IV compared to Type I. The effect of filling the tube

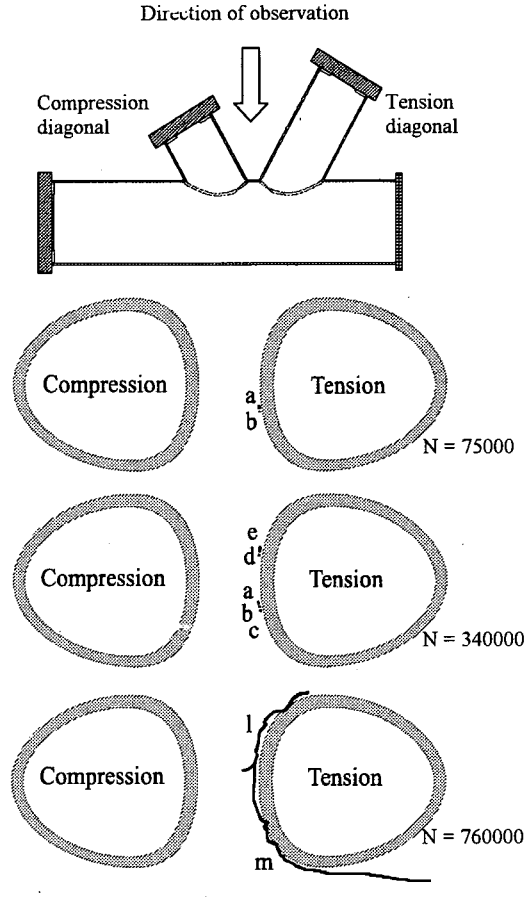

Fig.12 Fatigue crack development of the specimen KF-1

with concrete is to stiffen the joints by reducing the amount of ovalization and local deformation.

The most reduction in the stresses can be achieved by the model Type IV joint (with concrete) that combines the beneficial gains of filled concrete and perfobond stiffeners. To identify the influence of the perfobond stiffeners, the model Type IV (without concrete) represents Type IV joint without concrete filling. From **Fig.11**, it can be said that by providing perfobond stiffeners solely, reduction of the stress concentration is almost equal to Type II joints near the tension diagonal. However, at near the compression diagonal, the compressive stresses are much higher than Type II (with concrete) and Type III (with concrete) joints. By providing the filled concrete together with the strengthen materials, it can considerably reduce the overall and local deformations of the chord wall.

Henceforth, the crown toe will be a pertinent location as giving the highest stress concentration

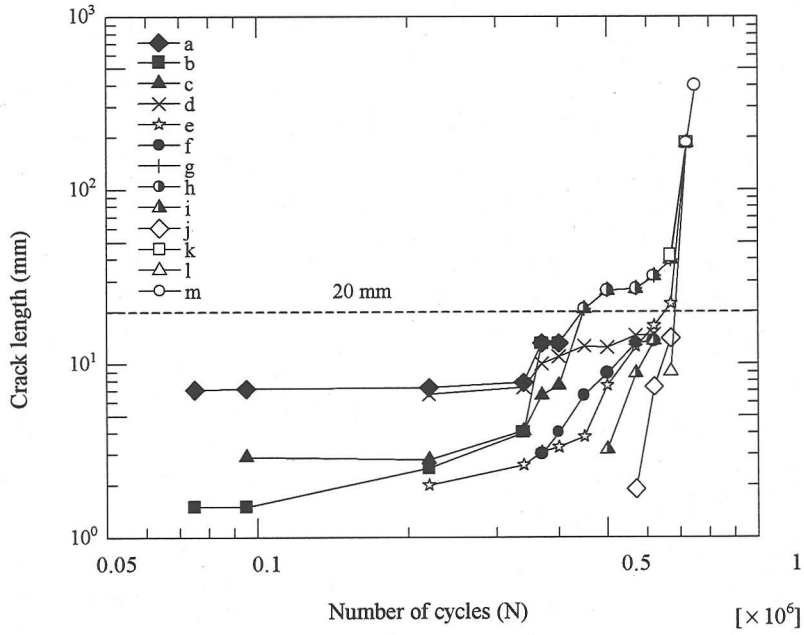

Fig.13 Crack length-number of cycles of the specimen KF-1

and will play a substantial role to the fatigue performance.

5. FATIGUE TEST RESULTS

(1) F atigue crack initiation and propagation

In almost all specimens, fatigue failure was primary associated with the tension diagonal from the fatigue cracking at the weld toe of the chord to the tension diagonal welds. The fatigue cracks initiated frequently at the inner crown positions and propagated along the weld toe around the weld circumference. Separate investigations and examinations of each joint type are described.

a) Type I (specimens KF-1, KF-3)

Fig.12 shows the fatigue crack initiation and fatigue crack development until failure of the specimen KF-1 as an example. Small cracks (a,b) initiated at the weld toe on the chord face of the chord to tension diagonal welds. These points of crack initiation were always located at the crown toe, which corresponded to the points where the maximum stresses were observed. The cracks, then, propagated along the weld circumference of the tension diagonal.

Fig.13 illustrates the fatigue crack propagation length versus number of cycles of the specimen KF-1. After a number of cycles, some new small cracks initiated. Consequently, the cracks coalesced to

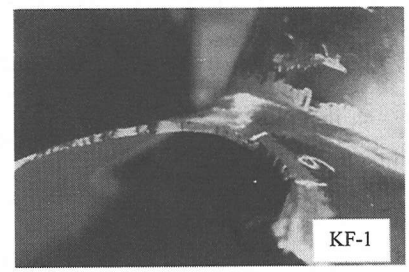

Fig.14 Failure of the specimen KF-1

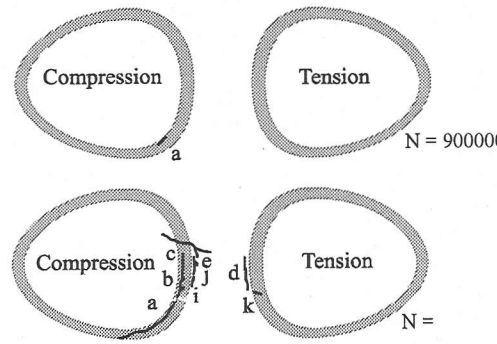

Fig.15 Fatigue crack development of the specimen KF-2

obtain a longer crack at almost the end of the fatigue life. It can be said that the observed first cracks do not propagate by itself through the end, but the other

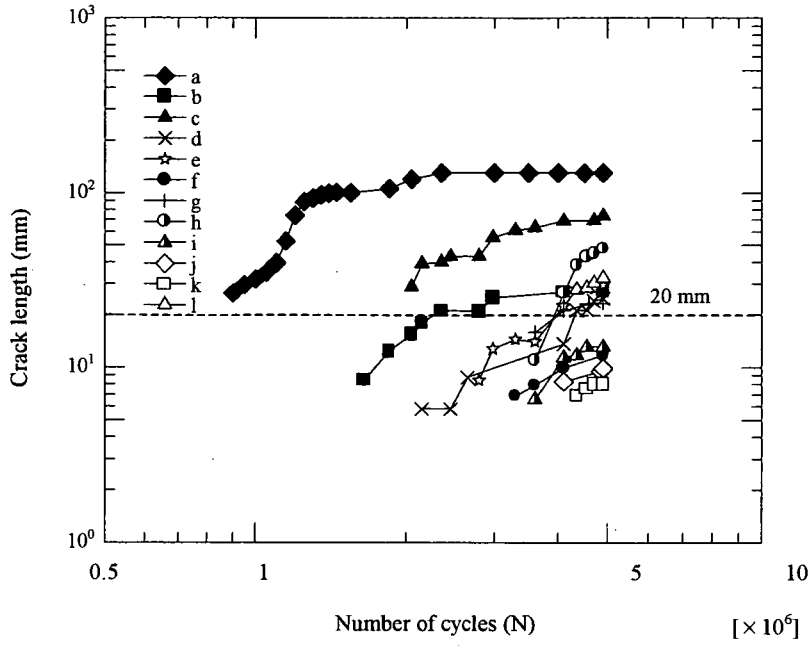

Fig.16 Crack length-number of cycles of the specimen KF-2

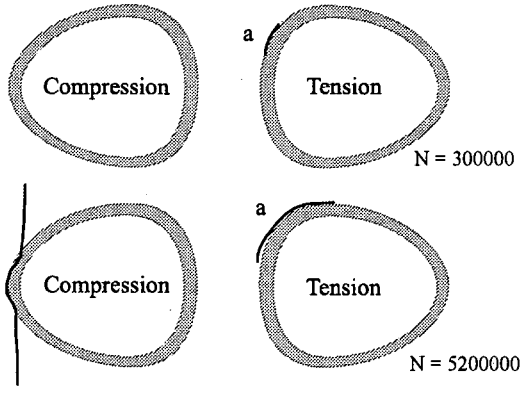

Fig.17 Fatigue crack development of the specimen KF-4

new surface crack initiation rather increases the total lengths of the crack. When the crack reached the saddle, it did not propagate along the weld circumference, but it propagated straightly on the chord wall. The crack propagation rate of the specimen KF-1 seems to be higher until reaching the failure and there was no crack near the compression diagonal. The failure could be observed as through thickness crack of the chord wall around the tension diagonal as shown in **Fig.14**.

b) Type II (specimens KF-2, KF-4)

Fig.15 shows fatigue cracks initiation on the weld root around compression diagonal of specimen KF-2. Although, the stress level at the compression diagonal are almost the same as the specimen KF-1

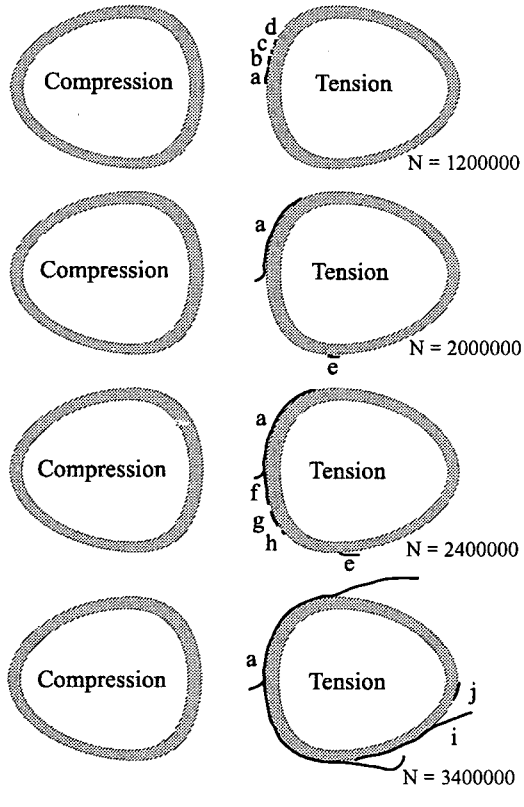

Fig.18 Fatigue crack development of the specimen KF-7

(see **Fig.10**). This phenomenon occurs due to the existing of residual stress at the weld. In addition, a

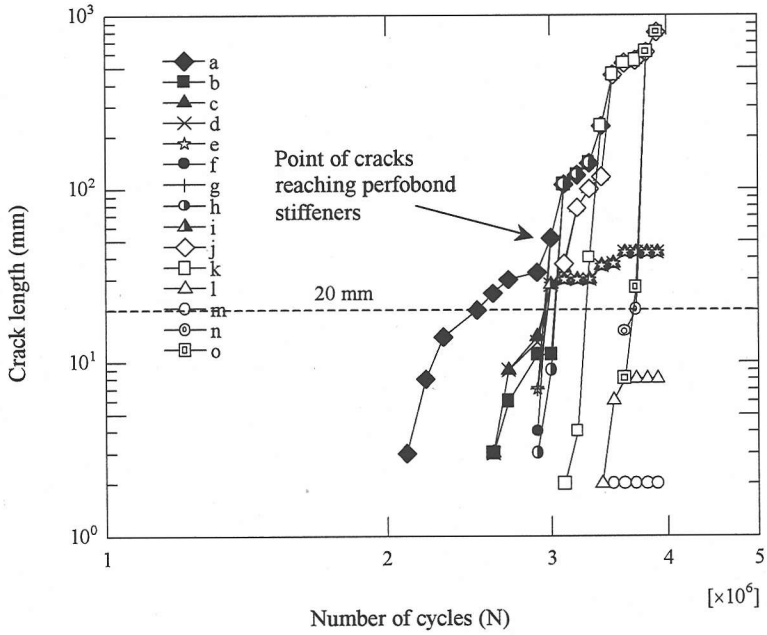

Fig.20 Crack length-number of cycles of the specimen KF-10

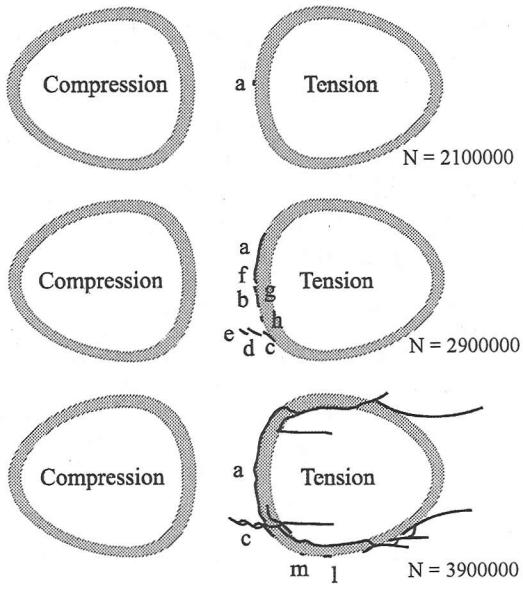

Fig.19 Fatigue crack development of the specimen KF-10

combination of bending stress and residual stress can result in tensile stress at the compression diagonal. It is noted that this phenomenon could not be observed in other specimens and it might have been caused by an initial imperfection of the test specimen.

Fig.16 illustrates the fatigue crack propagation length versus number of cycles of the specimen KF-2. It can be seen that at higher number of cycles,

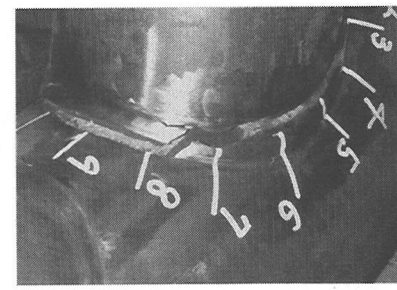

Fig.21 Failure of the specimen KF-10

crack propagation rate is slower and quite stable since the stress at tip did not increase. The stress range occurrence will not induce further fatigue crack if the resultant of the stress range is in compression. The longest fatigue crack length at the end of the test was about a quarter of intersection circumference as shown in **Fig.15**.

In specimen KF-4 as shown in **Fig.17**, fatigue cracks initiated at the location between crown toe and saddle of tension diagonal, and also at crown heel of compression diagonal. These two locations correspond to the high stress concentration locations. The failure of this specimen was observed as vertical chord wall fracture and some fatigue cracks at the tension diagonal.

c) Type III (specimens KF-6, KF-7, KF-9)

Crack propagation patterns of these specimens were quite similar to Type I joint. **Fig.18** illustrates fatigue crack propagation patterns of the specimen

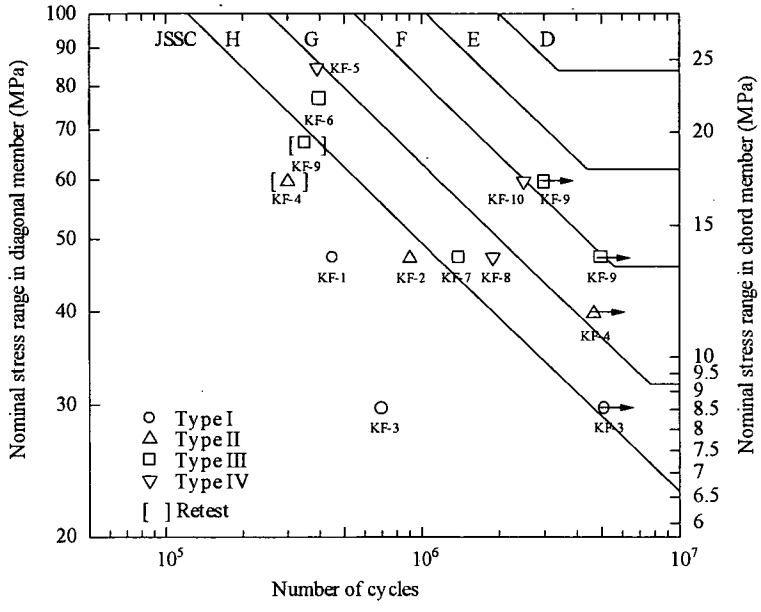

Fig.22 Nominal stress range-fatigue life, N_{20}

KF-7. Fatigue crack initiation life of this specimen occurred almost at the failure life of the specimen KF-1 (Type I). The first coalescence of some cracks occurred around 2000000 cycles where the second was nearly at the end of failure life.

d) Type IV (specimens KF-5, KF-8, KF-10)

Multiple cracks usually initiated and propagated along the intersection circumference of Type IV as similar to Type I, II, and III joints. Coalescing of cracks to obtain a longer crack could be seen in almost every specimen type.

In the specimen Type I and III, the longer crack obviously penetrated straight through the thickness of the chord wall when it reached the saddle. On the other hand, for Type IV, specimen KF-10 as an example, the development of the fatigue crack was different due to the presence of perfobond stiffeners as shown in **Fig.19** and **Fig.20**. The perfobond stiffeners acted as a crack arrester. When the crack reached the perfobond stiffeners, the crack changed its propagation direction through the weld bead, and propagated along the stiffener welds beneath tension diagonal and also on the weld circumference of the diagonal side. As shown in **Fig.21**, the failure at this state could be observed as ripping of the chord wall beneath the tension diagonal and weld root cracking.

(2) Fatigue performance based on nominal stress range

The results of all fatigue tests are listed in **Table 3**. These results correspond to the number of cycles which the surface fatigue crack lengths were observed and measured during the tests. The number of cycles to surface visible fatigue crack is denoted as N_c, the number of cycles to fatigue crack length 20 mm on the chord surface is denoted as N_{20} (assumed to be through thickness crack and taken as fatigue life) and the number of cycles to fatigue life at complete failure is denoted as N_f. Besides, the fatigue crack propagation life, N_p, is defined as the difference between the failure life (N_f) and the initiation life (N_c).

Fig.22 shows the relationships between nominal stress range of tension diagonal, S_n, and fatigue life, N_{20}, plotted against JSSC design curves[19]. The fatigue strengths of the joints Type I and II are lower than the JSSC-H design curve where Type III and IV are above or almost equal to the curve.

It is clear that the fatigue life of the improved joints Type II, III and IV are considerably greater than Type I owing to the effects of filled concrete. The concrete acts like a stiffener to restrain local deformation of the chord wall and enhances longer fatigue life. Regardless of the weld toe treatment, the specimen KF-7 (Type III) and KF-8 (Type IV) still give higher fatigue life than the treated specimen KF-2 (Type II) and KF-1 (Type I). By grinding, it can improve fatigue strength one or two classes higher as can be seen from the specimen KF-9 (Type III) and KF-10 (Type IV). When compared with as-welded specimen KF-7 (Type III) and specimen KF-8 (Type IV), Type IV joint provides higher fatigue life about 35%. In contrast, by improving the weld toe profile, the specimen KF-9

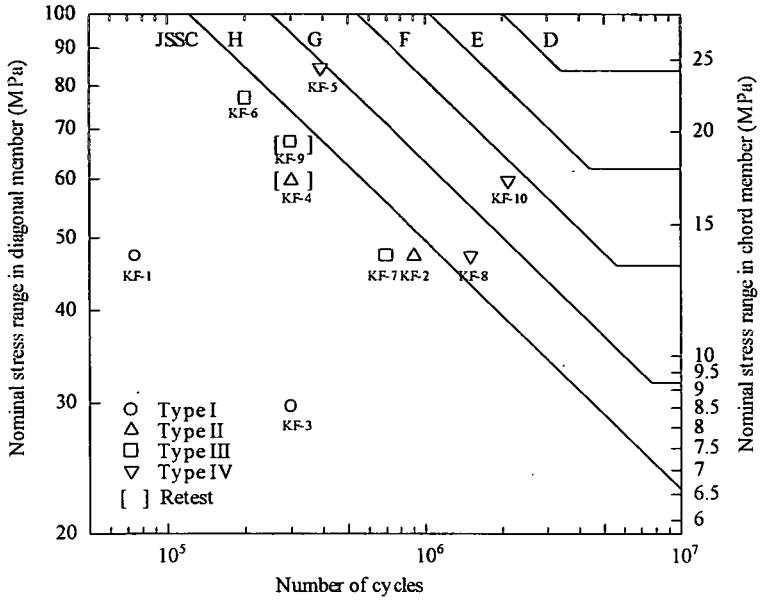

Fig.23 Nominal stress range-initiation life, N_c

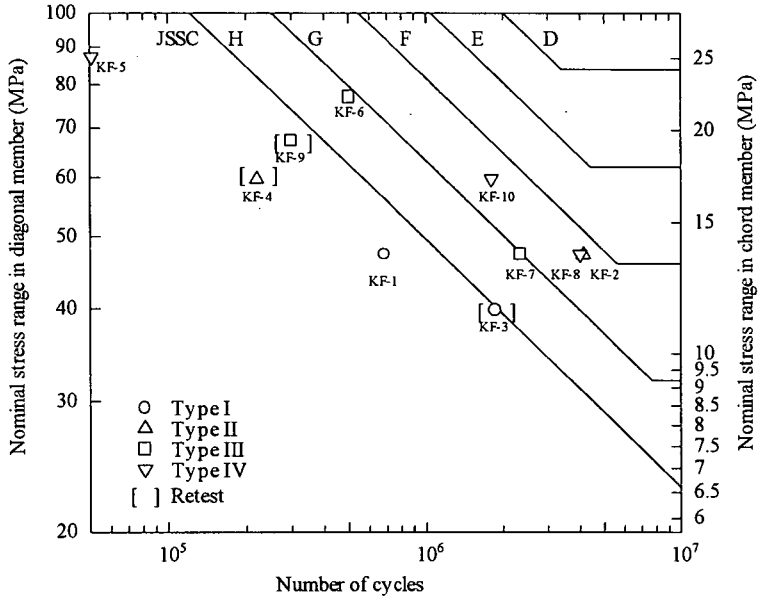

Fig.24 Nominal stress range-propagation life, N_p

(Type III) has longer fatigue life than the specimen KF-8 (Type IV) and KF-10 (Type IV) at least by 233% and 43%, respectively.

Fig.23, Fig.24, and **Fig.25** illustrate the relationships between the nominal stress range S_n-N_c (initiation life), S_n-N_p (propagation life), and S_n-N_f (failure life), respectively. In **Fig.23**, Type I joints (KF-1, KF-3), the fatigue cracks initiated at the weld toe faster than those three types. This was basically due to the highest stress concentration at the toe. The improved joints Type II, III and IV increase resistance to the fatigue crack initiation, especially on Type IV joints.

Accordingly, in **Fig.24**, the scatter of propagation lives of all joints is narrower than the initiation lives as in **Fig.23**. This indicates that the effectiveness of the joint improvement effect predominantly to the initiation life. In addition, the increases in crack

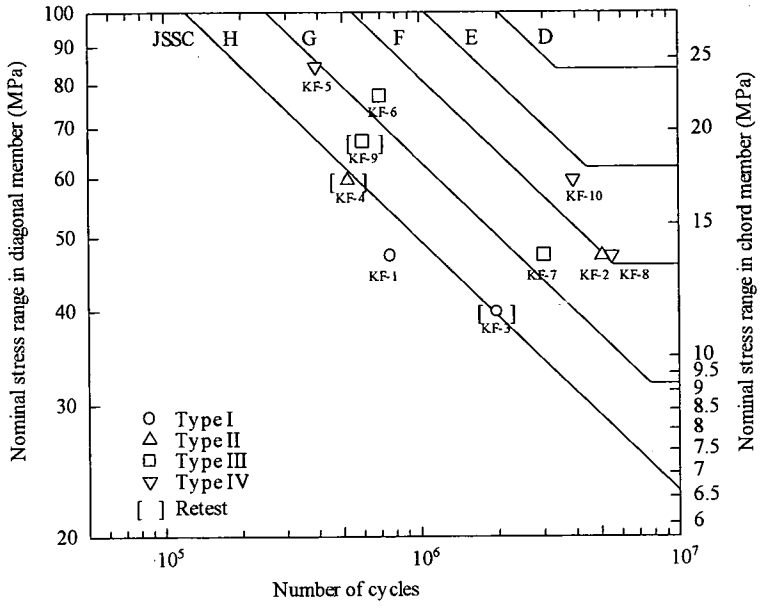

Fig.25 Nominal stress range-failure life, N_f

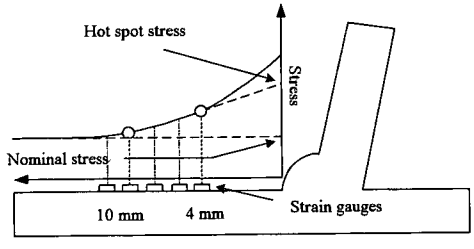

Fig.26 Extrapolated hot spot stress

propagation lives of the improved joints can be observed in this figure. However, at high nominal stress range level, Type IV (KF-5) specimen failed quickly as similar failure pattern to Type IV (KF-10) specimen without any notification of crack initiation.

(3) Fatigue performance based on hot spot stress range

In this study, as illustrated in **Fig.26**, hot spot stress was defined as the value extrapolated to the weld toe using the straight line connecting the stresses at 4 and 10 mm away from the weld toe.

The fatigue-resistant design of tubular joints is mainly based on hot spot stress range(S)-fatigue life(N) approach in which the fatigue life is obtained at different hot spot stress ranges using standard S-N curves recommended by various codes of practice. **Fig.27** and **Fig.28** show the fatigue performance (N_{20}) based on hot spot stress approach plotted against JSSC-E design curve for the as-welded joint specimens and JSSC-D design curve for the ground joint specimens. It is difficult to distinguish the fatigue performances of one joint type from those of the other types. This verifies our assumptions that hot spot stress concentration provides a common basis and it does not depend on the joint types. Also, scatters of the data on both as-welded and ground specimens are smaller than those of nominal stress basis.

According to the results, the fatigue strengths of the as-welded specimens can satisfy the JSSC-E class by using hot spot stress approach. When providing weld toe treatment by grinding, fatigue strengths of the joint have a tendency to be increased and satisfy the JSSC-D class. Accordingly, fatigue assessments of the tubular joints by using JSSC-E class for as-welded joint and JSSC-D class for ground joint can possibly be applied when the hot spot stress is defined as it is in this study.

6. IMPROVED JOINT ACHIEVEMENTS AND CONSIDERATIONS

Filling the tube with concrete is one alternative method to improve fatigue performance of conventional hollow joints. The achievements of the fatigue performance on each joint type can be roughly seen through the reduction of stress concentration.

In authors' point of view, Type IV joint provides the best fatigue performance among those four types based on the fatigue performance gains. The

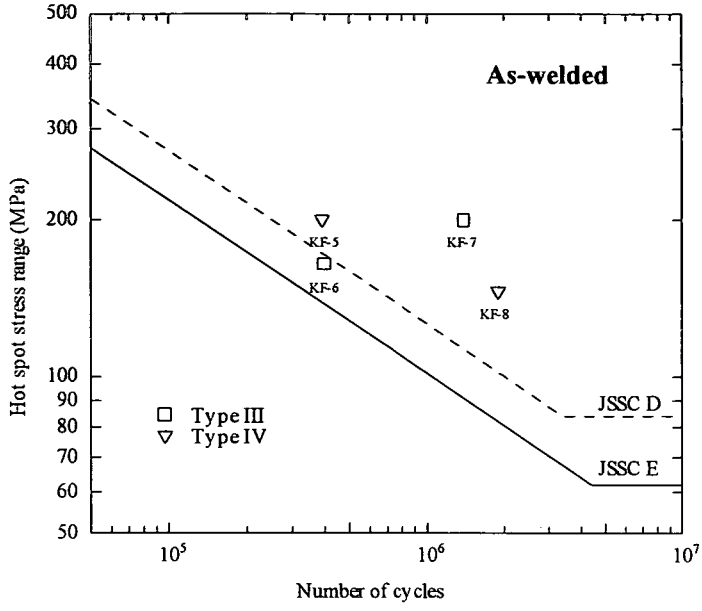

Fig.27 Hot spot stress range-fatigue life, N_{20}

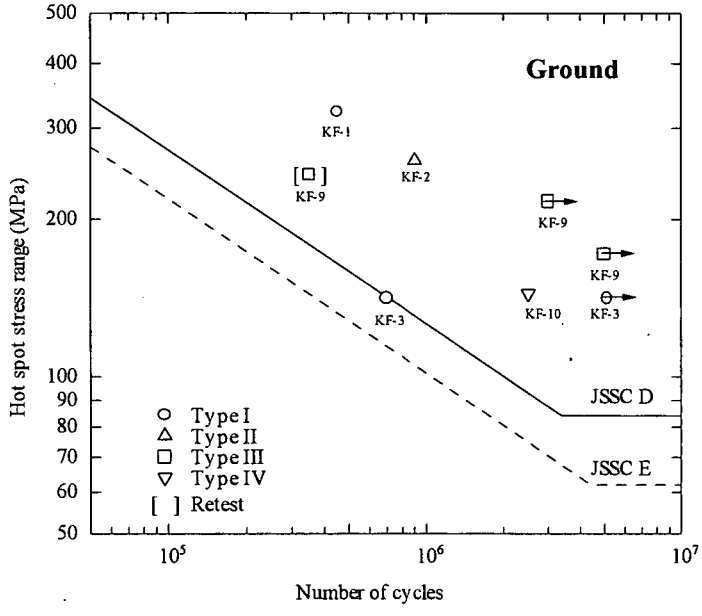

Fig.28 Hot spot stress range-fatigue life, N_{20}

presence of perfobond stiffeners tends to increase the initiation life by suppressing the stress concentration at the crown toe. Furthermore, they act as crack arresters to stop the cracks or to decelerate the propagation speed. This can improve the propagation life.

In order to apply Type IV joint to the bridge structure, the size effect due to different scale should be taking into consideration. It must not be considered in the evaluation by hot spot stress, but it must be considered in the evaluation by nominal stress. And also the different in tube wall thickness

is thought to be a source of different in fatigue strengths. The effect of steel plate thickness[19] must be considered in both evaluations. In addition, a special care must be made when it is subjected to high stress range level as being observed in the specimen KF-5. Ripping failure of weld root may be dangerous and relates directly to fatigue crack propagation life.

7. CONCLUSIONS

The improved joint technology presented in this paper provides the methods and assessments to strengthen simple tubular K-joint by upgrading structural joint details. Based on the investigations, the following conclusions are made:

1. The effect of filled concrete and perfobond stiffeners reduce the stress concentration by constraining chord wall deformation.
2. Fatigue crack propagation behavior of the joints depends on the structural joint details. The propagation patterns are different when the structural joint details are changed.
3. Fatigue performances of the improved joints Type III and IV satisfy the JSSC-H class based on nominal stress range basis. The effectiveness of weld toe treatment by grinding increases fatigue strength one or two classes higher.
4. Regardless of the joint types, fatigue assessment of the tubular joints by using JSSC-E class for as-welded joint and JSSC-D class for ground joint are applicable when the hot spot stress is defined as it is in this study.

ACKNOWLEDGEMENT: The authors gratefully acknowledge the supports of Mr. Anami K., Mr. Sasaki E. and Mr. Sakamoto T., Tokyo Institute of Technology.

REFERENCES

1) Marshall, P.W.: *Design of Weld Tubular Connections*, Elsevier Publishers, 1992.
2) Rao, A.G. Madhava and Raghava, G.: An Overview of Offshore Structures, Fatigue in Offshore Structures Book, Edited by Dover, W.D., and Rao, A.G. Madhava, Balkema Publishers, 1996.
3) Wardenier, J., Kurobane, Y., Packer, J.A., Dutta, D., and Yeomans, N.: Design Guide for Circular Hollow Section Joints Under Predominantly Static Loading, CIDECT, 1991.
4) Tajima, J., Takena, K., Miki, C., and Ito, F.: Fatigue Strengths of Truss Made of High Strength Steels. *Proc. of JSCE*, No. 341, January, 1984.
5) Miwa, H., Nagasawa, T., Yoda, T., Suzuki, T., and Kumagai, Y.: Experimental Study on the Mechanical Behaviour of Panel Joints in PC Hybrid Truss Bridges, *Journal of Structural Engineering*, JSCE, Vol.44A, pp. 1475-1483, 1998.
6) Pacific Consultants: Technical Reports on Tubular Truss Bridge, 1999.
7) Kurobane, Y.: Fatigue Strength of Tubular K-joints S-N Relationships Proposed as Tentative Design Criteria, IIW-XV-340-73, 1973.
8) Maeda, T., Uchino, K., and Sakurai, H.: Experimental Study on the Fatigue Strength of Welded Tubular K-Joints, IIW-XV-269-69, 1969.
9) Ohtake, F., Sakamoto, T., Tanaka, T., Kai, T., Nakazato, T., and Takigawa, T.: Static and Fatigue Strengths of High Tensile Strength Steel Tubular Joints for Offshore Structures, OTC 3254, 1978.
10) Teramoto, S., Kawasaki, T., Kaminokado, S., and Matoba, M.: Fatigue Strength of Welded Tubular Joints in Offshore Structures, *Mitsubishi Heavy Industries Technical Reports*, 1975.
11) Health & Safety Executive: Background to New Fatigue Guidance to Steel Joints and Connections in Offshore Structures, 1999.
12) Brown, G.M., Holmes, R., and McCann, D.L.: Improving Structural Integrity by Injection of Grout into Fatigue-Critical Nodes in Offshore Structures, OTC 5984, 1989.
13) Meur, G.L., Falcimaigne, J., and Ozanne, P.: Ultimate Strength and Fatigue Resistance of Grouted Tubular Joint, OMAE, 1994.
14) Silva, B., Carrol, B., Rosenberge, K., and Cladwell, D.: Testing of a New Grout Joint for Offshore Platforms, OTC 8829, 1998.
15) Packer, J.: Concrete-Filled HSS Connections, *Journal of Structural Engineering*, Vol. 121, No.3, pp. 458-467, 1995.
16) Railway Technical Research Institute: Design Standard for Railway Structures (Steel Railway Bridge and Composite Girder Railway Bridge), 1992.
17) Uchino, K. Sakurai, H., and Sugiyama, S.: Experimental Study on the Fatigue Strength of Welded Tubular K-joints, 2nd Report of the Joint Eccentricity on the Fatigue Strength, IIW-XV-344-73, 1973.
18) Hibbitt, Karlsson and Sorenson Inc.: ABAQUS User's Manual, Version 5.8, Providence, RI, 1998.
19) JSSC: *Fatigue Design Recommendations for Steel Structures*, 1995.

(Received May31, 2001)

コンクリートを充填した鋼管トラス橋K型格点部の疲労特性

Pison Udomworarat・三木千壽・市川篤司・古明地正典
・光木香・保坂鐵矢

本研究では，実際に建設が予定されている鋼管トラス橋に用いる，コンクリートを充填したK型格点部の構造特性について検討した．特に，構造ディテールおよび溶接止端部形状の改善による鋼管トラス格点部溶接継手部の疲労強度向上効果について実験的な検討を実施した．ここでは，10体の供試体を用意し，それらの挙動を実験結果およびFEM解析に基づいて検証した．その結果，コンクリートを充填した格点部の疲労強度は充填しない場合と比べて明らかに向上すること等が明らかとなった．